

Adiabatic optical entanglement between electron spins in separate quantum dots

S. K. Saikin,^{1,2,*} C. Emary,³ D. G. Steel,⁴ and L. J. Sham¹

¹*Department of Physics, University of California, San Diego, La Jolla, CA 92093*

²*Department of Physics, Kazan State University, Kazan 420008, Russian Federation*

³*Institut für Theoretische Physik, TU Berlin, Hardenbergstr. 36, D-10623, Germany*

⁴*Department of Physics, The University of Michigan Ann Arbor, MI 48109-1040*

(Dated: December 1, 2018)

We present an adiabatic approach to the design of entangling quantum operations with two electron spins localized in separate InAs/GaAs quantum dots via the Coulomb interaction between optically-excited localized states. Slowly-varying optical pulses minimize the pulse noise and the relaxation of the excited states. An analytic “dressed state” solution gives a clear physical picture of the entangling process, and a numerical solution is used to investigate the error dynamics. For two vertically-stacked quantum dots we show that, for a broad range of dot parameters, a two-spin state with concurrence $C > 0.85$ can be obtained by four optical pulses with durations $\sim 0.1 - 1$ ns.

PACS numbers: 78.67.Hc, 42.50.Ex, 03.67.Bg

Adiabatic passage uses the slow variation of a system’s Hamiltonian to select a particular quantum path while avoiding unintended dynamics. Controlled adiabatic evolution of the ground state has been proposed as a model for quantum computation.¹ Stimulated Raman adiabatic passage (STIRAP)² can be used to transfer populations or coherences between quantum states through a “dark state” which efficiently suppresses relaxation. Arbitrary single-qubit operations can be produced, for example, by STIRAP in a tripod system³ or adiabatically controlled Raman excitation in a Λ -system.⁴ In this work we study how adiabatic control can be used in design of optically-induced two-qubit quantum operations.

In systems with a permanent interaction between qubits, it is known that adiabatic passage through degenerate dressed states can also be used to construct two-qubit entangling gates.⁵ However, for scalable solid-state quantum computation, it is important to keep the qubits isolated from each other except during gating. Electron spins in semiconductor quantum dots (QDs) are promising candidates for just such qubits.⁶ They have long coherence time,⁷ can be manipulated by electric gates⁸ or optically,^{9,10} and the coupling between the qubits can be induced externally.

Significant experimental and theoretical effort has been invested in optical manipulation of electrons in single and coupled semiconductor QDs. Schottky diode structures with embedded self-assembled QDs have been designed to control the number of electrons in the dots by adjusting the external bias voltage.¹¹ The particular optical transitions between the charged and the excitonic states can be addressed in these dots by frequency and polarization selection.¹² Efficient spin-initialization schemes have been demonstrated recently using optical pumping in the Faraday¹³ (magnetic field parallel to the optical axis) and the Voigt¹² (magnetic field orthogonal to the optical axis) configurations. The Faraday¹⁴ and the Kerr¹⁵ rotations from single spins confined in QDs have been observed, which should allow spin-readout and single-spin rotation operations. For two-qubit quantum operations

the energy level structure and the interdot coupling in vertically-aligned QD pairs have been studied.^{16,17}

Several designs of two-qubit gates have been recently proposed utilizing, for example, tunneling between excited states of QDs,¹⁸ Förster-type interaction¹⁹ long-range coupling through a photon bus,²⁰ and electrostatic coupling between the excited states.^{21,22} These schemes are yet to demonstrated experimentally, however. The major difficulties are:

- The proposals utilize properties of the QDs or device structures which do not exist yet. For instance, two-qubit gates in Ref. 20 utilize QDs in cavities coupled to a common waveguide. Though, such a design could potentially allow large spatial separation of the qubits there are no reliable device structures yet.
- The interdot coupling via, for example, electron tunneling between the excited orbitals, or a Förster-type interaction requires precise alignment of the energy levels and cannot be controlled experimentally at the present stage of technology.
- Demonstration of a two-qubit operation is complicated because of the gate structure. Though, mathematically all the two-qubit entangling gates are equivalent, their physical realization, demonstration and implementation into a particular quantum algorithm require different amount of resources. It is particularly important when the operational noise is a main limiting factor. For instance, demonstration of conditional phase operation additionally involves a number of single qubit gates that themselves are very noisy and require a substantial experimental effort.

In this study we present a general approach to the design of two-qubit entangling operations with *uncoupled* electron spins in semiconductor QDs utilizing the Coulomb interaction of transient optically-excited states localized in the dots. We show that adiabatic pulses combined with the counter-intuitive pulse ordering of STIRAP allows the construction of non-local two-spin unitary transformations, whilst efficiently suppressing population transfer out of the qubit subspace. Compared to

other two-qubit gates with spins in semiconductor QDs our proposal:

- utilizes the conventional Schottky barrier device structures within which QDs are routinely grown;
- is based on the Coulomb interaction between the excited electronic states in different dots, and therefore does not require precise control for the energy level structure;
- provides flexibility in the gate design. In addition to control phase gates one can construct operations resulting in a coherent oscillation of two-spin state populations which is a more accessible signature of entanglement.

As illustration we describe an operation for two spins in separate self-assembled InAs/GaAs QDs. While, for clarity, the entangling process is described in the pulse language, it, in fact, represents a quantum operation made up of a product of \sqrt{i} SWAP and controlled-phase gates. Combined with single qubit rotations⁴ and optical initialization,^{12,23} we obtain a set of gates for universal quantum computation. We employ the Voigt configuration to obtain the flexibility required to select the desired quantum paths through polarization and frequency selection. The evolution of the system is then guided through a particular subset of quantum paths by a sequence of adiabatic pulses. In our dressed-state picture the scheme can be viewed as an adiabatic passage of an arbitrary initial two-spin state through two long-lived states. The interference between the two paths results in an effective rotation in the spin subspace. The method proposed here can be adapted to construct CPHASE and CNOT gates.

In two self-assembled InAs/GaAs QDs, the direct electron or hole tunneling between the dots may be suppressed by selecting the dot heights and the interdot distance.^{16,18} Then, because the electrons and holes are confined differently, the intrinsic Coulomb coupling between particles in different dots modifies the optical transition energies.^{16,17} We employ this phenomenon to perform two-qubit operations. This is similar to the dipole blockade.²⁴ However, we do not rely on an external electric field. This substantially simplifies the experimental setup and makes the operation less sensitive to external noise than the proposal of Ref. 21 in which in-plane gates were used. The particular path used for the entangling operation is shown in Fig. 1(a). In the ideal case of strong Coulomb interaction, starting with the polarized state $|+, +\rangle$ one obtains the maximally entangled state $\frac{1}{\sqrt{2}}(|+, +\rangle + i|-, -\rangle)$ after an effective $\pi/2$ two-spin rotation. A longer excitation pulse results in coherent oscillations between $|+, +\rangle$ and $|-, -\rangle$ populations — an experimentally observable signature of the entanglement between the spins. Schematics of the pulse sequence and of the evolution of the appropriate dressed states are shown in Fig. 1(b,c). The long optical pulses used here may be generated by modulating cw lasers, which would provide sufficiently narrow frequency spectra of the pulses. Coherent optical coupling of the 5-state system shown in Fig. 1(a) does not yield a dark state, unlike in the familiar Λ system. However, the two states we use are long-lived under two-photon resonance,²⁵ and we can

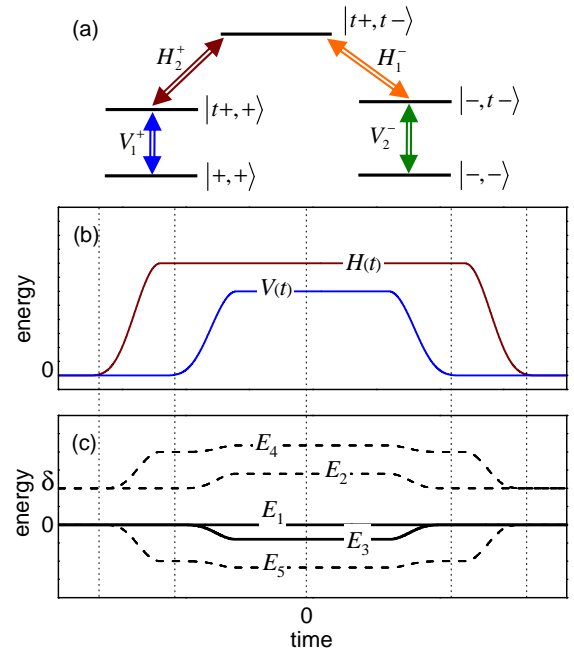


FIG. 1: (Color online) (a) Optical scheme to control the entanglement between spins in two InAs/GaAs QDs in the Voigt configuration. Two-dot states are denoted by kets such as $|t\pm, \pm\rangle$, with $|\pm\rangle$ for the spin states and $|t\pm\rangle$ the trion states. Arrows indicate the linear polarizations V_j^\pm and H_j^\pm for the transitions $|\pm\rangle \leftrightarrow |t\pm\rangle$ and $|\pm\rangle \leftrightarrow |t\mp\rangle$ of dot $j = 1, 2$. (b) Timing of pulses for either dot. $V(t)$ and $H(t)$ are envelope functions, for which we use the same shape, rectangular with fronts shaped as $\sin^4(\pi t/T_j)$, for all pulses, and the same amplitudes for both V-pulses and for both H-pulses. (c) Adiabatic time evolution of the dressed state energies. Solid lines show the essential energies which drive the operation.

further reduce trion relaxation by detuning the optical pulses and by adjusting their amplitudes.

For a single QD in the Voigt configuration with two single-electron spin states

$$|\pm\rangle = \frac{1}{\sqrt{2}}(e_{\downarrow}^\dagger \mp e_{\uparrow}^\dagger)|0\rangle, \quad (1)$$

we consider only two lowest-energy negative-trion states

$$|t\pm\rangle = \frac{1}{\sqrt{2}}e_{\downarrow}^\dagger e_{\uparrow}^\dagger (h_{\uparrow}^\dagger \mp h_{\downarrow}^\dagger)|0\rangle, \quad (2)$$

where the operators $e_{\uparrow, \downarrow}^\dagger$ and $h_{\uparrow, \downarrow}^\dagger$ create, respectively, an electron and a heavy hole with spin along or against the growth direction, which we also take as the optical axis. Because of the large confinement splitting, the heavy hole is only weakly mixed with the light hole, and this can be easily compensated for by adjusting polarizations of the optical fields.⁴ With these restrictions, the system of two dots has 16 states. The four lowest energy spin states form the qubit sector. They are separated by a gap from eight single-trion states, which are similarly distant from four bi-trion states. The interdot Coulomb interaction of

electrons and holes gives rise to a binding energy of the bi-trion,

$$\Delta = E_{1221}^{eeee} + E_{1221}^{hhhh} - E_{1221}^{ehhe} - E_{2112}^{ehhe}, \quad (3)$$

where E_{jkkj}^{abba} is a two-particle Coulomb integral, e or h denotes electron or hole and $j = 1, 2$ labels the dots, and we assume that the interdot electron-hole exchange is negligible due to the large distance. In zero magnetic field, let the transition energy from the qubit sector to the single-trion sector be ω_{tj} . The single- to bi-trion transition energy is shifted by the binding energy Δ , thus enabling the two types of transition to be independently addressed. Four optical fields can thus couple the states $|+, -\rangle$ and $|-, +\rangle$, or states $|+, +\rangle$ and $|-, -\rangle$. In the following we use the latter pair because an efficient initialization of the state $|+, +\rangle$ is possible.¹²

Firstly, we develop an analytic model describing the two-qubit gate. It assumes strong Coulomb interaction between the trions and does not account for relaxation from the excited states. These assumptions are relaxed later using numerical simulations of the system's dynamics.

The essential process of the quantum operation can be described by a Hamiltonian

$$H = \begin{pmatrix} 0 & V_1^*(t) & 0 & 0 & 0 \\ V_1(t) & \delta & H_1^*(t) & 0 & 0 \\ 0 & H_1(t) & 0 & H_2(t) & 0 \\ 0 & 0 & H_2^*(t) & \delta & V_2(t) \\ 0 & 0 & 0 & V_2^*(t) & 0 \end{pmatrix}, \quad (4)$$

acting on the five-level system, Fig. 1(a), written in the rotating wave approximation and an interaction picture. The stationary basis states of the Hamiltonian are $|+, +\rangle$, $|t+, +\rangle$, $|t+, t-\rangle$, $|-, t-\rangle$, and $|-, -\rangle$. The optical fields are detuned by δ from the single-trion transitions to avoid populating the intermediate states, while the two-photon processes are resonant with the bi-trion transition. For the sake of simplicity we use the same shape for both H-pulses and both V-pulses. We therefore omit the indices of the pulse envelopes in Eq. 4 in the following discussion. The two H-polarized pulses create the interaction between two dots by optically coupling the bi-trion state to two single-trion states in the dots. Then, the shorter V-polarized pulses couple the qubit sector to the renormalised excited states and rotate the spins in a way similar to the single qubit operation.⁴ The operation can be described in terms of dressed states, \mathbf{C}_{1-5} . In the adiabatic approximation for positive δ their energies are

$$\begin{aligned} E_1 &= 0, \\ E_{2,3} &= \frac{1}{2}(\delta \pm \sqrt{\delta^2 + 4V(t)^2}), \\ E_{4,5} &= \frac{1}{2}(\delta \pm \sqrt{\delta^2 + 4V(t)^2 + 8H(t)^2}), \end{aligned} \quad (5)$$

which are sketched in Fig. 1(c). Adiabatic pulses do not excite transitions to the split-off levels $E_{2,4}$, and thus states \mathbf{C}_2 , \mathbf{C}_4 may be ignored. The H-pulse is applied first and lifts the degeneracy of $E_{1,3}$ and E_5 levels, but

state \mathbf{C}_5 remains orthogonal to the spin subspace and thus the initial spin state is not transferred to it. The transformation of a spin-state is controlled only by the evolution of the states \mathbf{C}_1 and \mathbf{C}_3 , which can be written as

$$\begin{aligned} \mathbf{C}_1 &= -\frac{1}{\sqrt{2}}[\cos \theta, 0, -\sin \theta, 0, \cos \theta], \\ \mathbf{C}_3 &= -\frac{1}{\sqrt{2}}[\cos \varphi_1, -\sin \varphi_1, 0, \sin \varphi_1, -\cos \varphi_1], \end{aligned} \quad (6)$$

in terms of time-varying angles defined by

$$\tan \theta = \frac{V(t)}{\sqrt{2}H(t)}, \quad \tan 2\varphi_1 = \frac{2V(t)}{\delta}. \quad (7)$$

When the optical fields are switched off, \mathbf{C}_1 and \mathbf{C}_3 reduce to $\frac{1}{\sqrt{2}}[1, 0, 0, 0, \pm 1]$ which belong to the spin sector, $\mathbf{C}_{2,4}$ to single-trion states, and \mathbf{C}_5 to $|t+, t-\rangle$. The evolution of the spin states $|+, +\rangle$ and $|-, -\rangle$ is controlled by the unitary transformation $e^{-i\phi_1(1-\sigma_x)}$, where $\sigma_x = |+, +\rangle\langle -, -| + |-, -\rangle\langle +, +|$ and

$$\phi_1 = \frac{1}{2} \int E_3(\tau) d\tau, \quad (8)$$

where $\hbar = 1$ is assumed. An excitation with $\phi_1 = \pi/4$ would create a maximally entangled state from either $|+, +\rangle$ or $|-, -\rangle$. The operation is designed to minimize the effects of relaxation from excited states and pulse imperfections. The states \mathbf{C}_1 and \mathbf{C}_3 overlap within the qubit sector only. Therefore, the initial state always returns back to the qubit sector at the end of the operation. If a part of population is transferred to \mathbf{C}_5 , for example, by applying optical pulses simultaneously, the bi-trion state will be left populated. However, this can be minimized by detuning of the two-photon excitation processes from the bi-trion transitions. Also the populations of the excited state components of \mathbf{C}_1 and \mathbf{C}_3 are controlled by the small parameters $(V/\delta)^2$ and $(V/H)^2$. Below we show that it is possible to maintain the total population of the excited states below 10% for pulse durations of the order of 1 ns. This makes the lifetime of \mathbf{C}_1 and \mathbf{C}_3 about 10 times longer than that of bare trions. For an arbitrary initial state, in addition to two-spin rotation described above, the $|+, -\rangle$ state acquires a phase $e^{-i\phi_2}$, where

$$\phi_2 = \frac{1}{2} \int [\delta - \sqrt{\delta^2 + 8V(\tau)^2}] d\tau, \quad (9)$$

driven by the V-fields coupling to the single trions $|t+, -\rangle$ and $|+, t-\rangle$. The optically-induced transformation of an arbitrary two-spin state in the approximation of a strong Coulomb coupling and a large splitting between the Zeeman sublevels is

$$U_{\text{id}} = \begin{pmatrix} e^{-i\phi_1} \cos \phi_1 & 0 & 0 & ie^{-i\phi_1} \sin \phi_1 \\ 0 & e^{-i\phi_2} & 0 & 0 \\ 0 & 0 & 1 & 0 \\ ie^{-i\phi_1} \sin \phi_1 & 0 & 0 & e^{-i\phi_1} \cos \phi_1 \end{pmatrix}, \quad (10)$$

where the phases $\phi_{1,2}$ are defined by Eqs. (8) and (9) respectively.

Detuning the optical fields is required to avoid unintended dynamics, such as population transfer from $|+, -\rangle$ to the single trion states $|t+, -\rangle$ or $|+, t-\rangle$. As an aid to the design of this process, we gather in Fig. 2 all the transition energies for both polarizations. The input parameters are the energy levels from the dot fabrication, Δ from dot placement, the Zeeman splittings, and the central frequencies of the optical pulses parameterised by single detuning δ for simplicity. Correction operation constrains these parameters as

$$\Delta\omega_t \gg \Delta \gg \Pi_i, \Sigma_i \gg \delta, \quad (11)$$

which is physically reasonable. If the bi-trion binding energy Δ and the Zeeman splittings Π_i and Σ_i are comparable to the detuning δ , off-resonant processes have the undesired effect that the pulse sequence which excites the desired quantum path also excites a path involving the single trion states $|+, t-\rangle$ and $|t+, -\rangle$, albeit off-resonantly. This reduces the two-spin rotation angle. This secondary process can be investigated with a 5-level model similar to that of the resonant path. All other off-resonant excitations just give rise to phases in second-order perturbation. Including these effects, Fig. 10 can

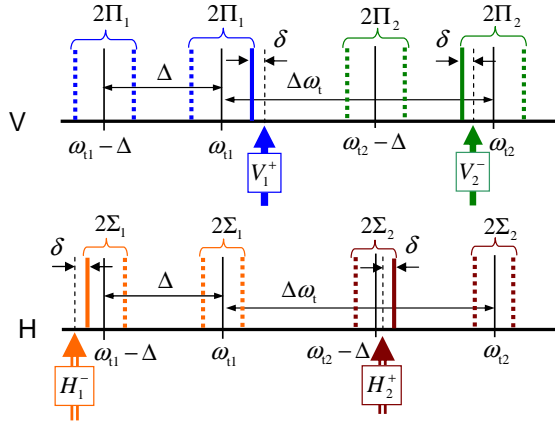


FIG. 2: (Color online) Energies of allowed optical transitions versus the optical frequencies (measured in energy units) for V-polarization (upper figure) and H-polarization (lower figure). The thin solid lines mark the transition energies in zero magnetic field. ω_{tj} is the transition energy between a spin state and a trion state in dot j . Their difference between the dots is shown as $\Delta\omega_t = \omega_{t2} - \omega_{t1}$. Δ is the bi-trion binding energy, thus making the transition energy between the single and bi-trion $\omega_{tj} - \Delta$. In a magnetic field, the electron and hole Zeeman splittings, ω_j^e and ω_j^h in dot j , cause the transition energy splitting, $2\Pi_j = \omega_j^e + \omega_j^h$ in the V-polarization and $2\Sigma_j = \omega_j^e - \omega_j^h$ in the H-polarization. The Zeeman splitted transitions used in the quantum operation and off-resonant transitions are denoted by the thick solid lines and thick dashed lines respectively. The vertical arrows show the central frequencies of the optical pulses and their detuning δ from the corresponding transitions.

thus be generalized as

$$U = \begin{pmatrix} e^{-i\phi_{11}} \cos \alpha & 0 & 0 & ie^{-i\phi_{14}} \sin \alpha \\ 0 & e^{-i\phi_{22}} & 0 & 0 \\ 0 & 0 & e^{-i\phi_{33}} & 0 \\ ie^{-i\phi_{41}} \sin \alpha & 0 & 0 & e^{-i\phi_{44}} \cos \alpha \end{pmatrix}, \quad (12)$$

where the phases ϕ_{ij} and α are defined in Appendix. Equation (12) is not a standard quantum gate. Its usefulness for quantum information processing has been discussed in Ref. 18. In general, the gate can be factorized as a product of control phase gates and a SWAP gate. Starting with an initially spin-polarized $|+, +\rangle$ or $|-, -\rangle$ state one can generate a maximally-entangled state with $\alpha = \pi/4$. Moreover, a longer excitation pulse should result in coherent two-spin oscillations.

To examine the effects of trion relaxation and off-resonant pumping, we numerically integrate the equation of motion for the 16-level density matrix including all transitions of Fig. 2. In particular, we consider two vertically-stacked InAs QDs. We model the trion relaxation with a Lindblad form,²³ and assume that all transitions are independent with the total relaxation rate $\Gamma = 1.2 \mu\text{eV}$.¹³ The recombination rate of electrons and holes in different dots, as well as their spin decoherence rate⁷ are negligible on the operation timescale. We take the interdot difference of the two single-trion energies to be $\Delta\omega_t = 10 \text{ meV}$, and the electron and hole g-factors to be $g_e = -0.48$, $g_h = -0.31$ ¹² for both dots. There appears to be no experimental data on the bi-trion binding energy in the literature. Gerardot et al. obtained 4.56 meV for binding energy of two excitons located in dots with a vertical separation 4.5 nm.¹⁶ Scheibner et al.¹⁷ measured -0.3 meV for the shift of a negative trion transition when a second dot is occupied by a hole with respect to a bare transition (interdot distance is 6 nm). These give us two disparate values for the biexciton binding energy. From a simple analytical model¹¹ we estimate $\Delta = 0.8 \text{ meV}$ for dots with vertical separation 8 nm. To characterize the entanglement of the output qubit state we use the concurrence, C .²⁶

The most crucial parameter of the operation is the bi-trion binding energy Δ . Figure 3 shows the concurrence of the output state as a function of Δ for several different excitations. The laser fields are weak enough to avoid unintentional dynamics outside the 16-level system (not studied here). We find that a state with a concurrence $C > 0.85$ can be generated if $\Delta \geq 0.3 \text{ meV}$ for a broad range of excitation parameters. The lower boundary for Δ is determined by the symmetry of the excitation scheme. One can see in Fig. 2 that if Δ is comparable to the Zeeman splitting the fields V_2^- and H_2^+ will excite transitions from the Coulomb-split doublets, in addition to the intended transitions. This effect is avoided if we design a gate to swap $|+, -\rangle$ and $|-, +\rangle$ states. In the latter case the concurrence of the gate remains $C > 0.85$ for $\Delta \geq 0.1 \text{ meV}$ and smoothly decays to zero at $\Delta \approx 10 \mu\text{eV}$.

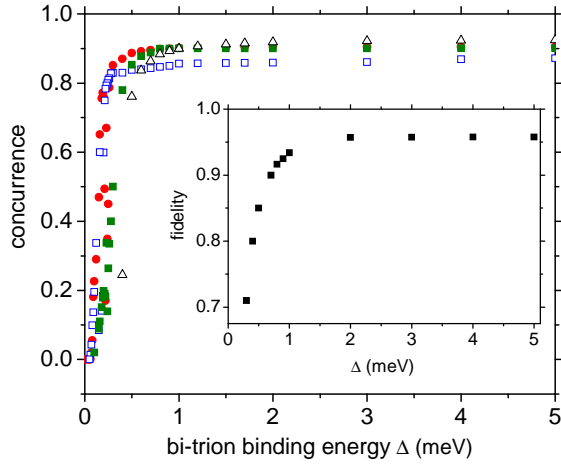


FIG. 3: (Color online) Concurrence of the output two-spin state for different bi-trion binding energies. Excitation parameters: filled circles – $\delta = -0.1$ meV, $V_0 = 20$ meV $H_0 = 44$ meV; open squares – $\delta = -0.13$ meV, $V_0 = 20$ meV $H_0 = 44$ meV; filled squares – $\delta = -0.1$ meV, $V_0 = 10$ meV $H_0 = 44$ meV; open triangles – $\delta = 0.12$ meV, $V_0 = 15$ meV $H_0 = 65$ meV. V_0 and H_0 denote amplitudes of the V- and H-polarized fields. Inset: fidelity of the analytical model compared to numerical simulations as a function of Δ .

The time required to entangle two spins is on the order of fractions of a nanosecond for the whole range of Δ . It is much shorter than the free-qubit decoherence time ($\sim 1\mu\text{sec}$) at low temperatures determined by the interaction with a nuclear spin bath.⁷ The main factors limiting the precision of an operation in this case are excitation of unintended transitions and relaxation from the optically excited states utilized in the scheme. Our approach allows precise control for unintended excitations. Within the 16-level model, if we assume an infinite relaxation time for the single- and bi-trion states, the population of the excited states, after the optical fields are turned off, is less than 10^{-5} . Variations in pulse shapes or field intensities do not affect this value. In this sense our adiabatic excitation scheme is more robust compare to fast resonant operations utilizing pulse-shaping. Although the effect of relaxation from the excited states in our scheme is strongly suppressed by detuning of optical fields it is still noticeable and limits the concurrence of a maximally-entangled state. To further reduce the relaxation effects one has to increase detunings of optical fields and use QDs with greater separation between the energy levels (stronger Zeeman splitting and larger Δ).

To characterize the precision of the designed operation we define a fidelity of the gate^{18,27}

$$F = \overline{\langle \psi_0 | (U')^\dagger \rho_f U' | \psi_0 \rangle}, \quad (13)$$

as it is described by our adiabatic analytic solution, Eq. (12), compare to numerical simulation of quantum dynamics of the 16-level system that includes non-adiabaticity effects and relaxation. The bar over Eq. (13) is for average over all initial states of two qubits, and ρ_f

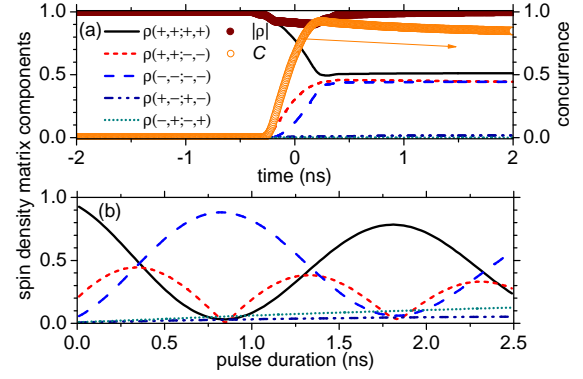


FIG. 4: (Color online) Evolution of a spin state controlled by four optical fields. The Coulomb coupling is $\Delta = 0.3$ meV, the detuning is $\delta = -0.1$ meV, the magnetic field is $B = 8$ T and the field amplitudes are $V_0 = 20 \mu\text{eV}$ and $H_0 = 44 \mu\text{eV}$. Durations of the H- and V-pulses interrelated as $T_H = T_V + 2T_f$, $T_f = 250$ ps is the front duration. (a) Optical pulses are centered at $t = 0$, $T_V = 340$ ps. The components not shown in the figure are below 10^{-3} at the end of the excitation. (b) Spin density matrix as a function of T_V .

is a two-qubit density matrix obtained in the numerical simulations. This is the most objective method to analyze the theoretical model short of having experimental data for comparison. The inset of Fig. 3 show that the analytical model provides a good description of the operation in the same range of Δ .

An example of an entangling two-qubit evolution is given in Fig. 4 for two dots with the Coulomb coupling $\Delta = 0.3$ meV. The optical pulses, centered at $t = 0$, have been optimized to obtain a final state with a maximal entanglement from $|+, +\rangle$. The output concurrence $C \approx 0.87$ is limited by relaxation from the single- and bi-trion states. However, because only a small part of population is transferred to the excited states the entangling operation is weakly sensitive to the trion relaxation rate: doubling it results in less than 10% variation of the concurrence. Longer excitation pulses result in Rabi oscillations of the pseudo-spin, Fig. 4(b), which is consistent with the analytic model. The decay time of the Rabi oscillations is of the order of 10 nanoseconds. The conventional 3D tomography plot, Fig. 5, shows the two-spin density matrix after the entangling gate is applied, compared with the ideal one obtained from Eq. (12).

To measure the entanglement of the output state in an experiment requires a full-state tomography,²⁸ which could be rather difficult and a discussion of which is outside the scope of this work. However partial indication is provided by the oscillations between states $|+, +\rangle$ and $|-, -\rangle$ under longer excitation, Fig. 4(b). This effect can be probed by exciting resonantly the population of a given spin state and then measuring absorption or fluorescence. With two optical fields, one can selectively excite a transition from a single two-spin state to a bi-trion state. For instance, optical fields V_1^+ and H_2^+ applied to the systems excite resonantly two-photon transition

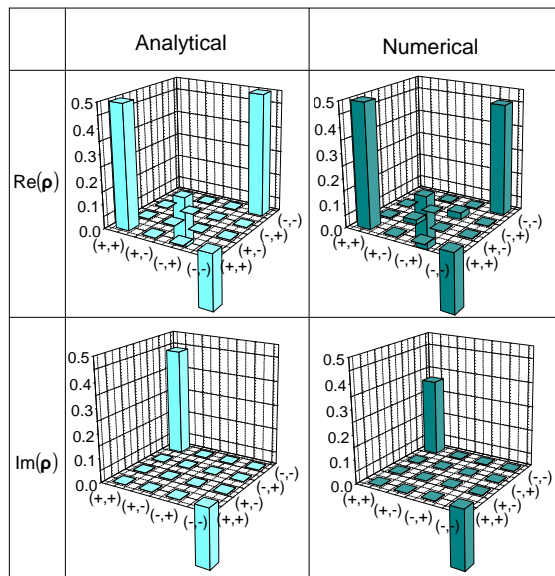


FIG. 5: (Color online) Density matrix of the output two-qubit state prepared from $|+, +\rangle$ using an optimised entangling gate. The analytic solution, obtained using Eq. 12, is compared with the numerical simulations. Parameters of the dots and the optical fields are the same as in Fig. 4.

between $|+, +\rangle$ and $|t+, t-\rangle$ states only, see Fig. 1(a). All other transitions are off-resonant. Therefore, fluorescence should be proportional to the population of $|+, +\rangle$. To confirm that the fields excite a two-photon transition one could measure two-photon cross correlations.¹⁶

In conclusion, we have developed an adiabatic approach for the optically-controlled entangling quantum operations with two electron spins in semiconductor self-assembled quantum dots. The scheme, utilizing the Coulomb interaction between trions, is insensitive to material parameters, pulse imperfections and trion relaxation. We show that using four optical fields a highly-entangled two-spin state with the concurrence $C > 0.85$ can be prepared on the timescale of the order of 1 ns.

Acknowledgments

This work was supported by ARO/NSA-LPS and DFG grant BR 1528/5-1. We thank Dan Gammon, Xiaodong

Xu, and Yuli Lyanda-Geller for helpful discussions.

APPENDIX A

The phases in the transformation matrix, Eq. 12, are defined as follows:

$$\begin{aligned} \alpha &= \phi_1 + \psi^-, \\ \phi_{11} &= \phi_1 + \psi^+ + \int h_1(\tau) d\tau, \\ \phi_{22} &= \phi_2 + \int h_2(\tau) d\tau, \\ \phi_{33} &= \int h_3(\tau) d\tau, \\ \phi_{44} &= \phi_1 + \psi^+ + \int h_4(\tau) d\tau, \\ \phi_{14} = \phi_{41} &= \phi_1 + \psi^+ + \int h^+(\tau) d\tau, \end{aligned}$$

where

$$\begin{aligned} \psi^\pm &= (\psi_1 \pm \psi_2)/2, \\ \psi_1 &= - \int \left[\frac{\Delta - \delta}{2} - \sqrt{\frac{(\Delta - \delta)^2}{4} + H^2(\tau) + 2V^2(\tau)} \right] d\tau, \\ \psi_2 &= - \int \left[\frac{\Delta - \delta}{2} - \sqrt{\frac{(\Delta - \delta)^2}{4} + H^2(\tau)} \right] d\tau, \end{aligned}$$

and

$$\begin{aligned} h_1(\tau) &= -\frac{V^2(\tau)}{2\Pi + \delta} - \frac{H^2(\tau)}{\Delta - \delta + 2\Sigma}, \\ h_2(\tau) &= \frac{V^2(\tau)}{2\Pi - \delta} - \frac{H^2(\tau)}{\Delta - \delta - 2\Sigma}, \\ h_3(\tau) &= -\frac{H^2(\tau)}{\Delta - \delta + 2\Sigma} - \frac{H^2(\tau)}{\Delta - \delta - 2\Sigma}, \\ h_4(\tau) &= -\frac{V^2(\tau)}{2\Pi + \delta} + \frac{V^2(\tau)}{2\Pi - \delta}, \\ h^\pm(\tau) &= h_1(\tau) \pm h_4(\tau). \end{aligned}$$

* saykin@fas.harvard.edu

¹ E. Farhi, J. Goldstone, S. Gutmann, J. Lapan, A. Lundgren, and D. Preda, *Science*, **292**, 472 (2001).

² J. Oreg, F. T. Hioe, and J. H. Eberly, *Phys. Rev. A* **29**, 690 (1984); K. Bergmann, H. Theuer, B. W. Shore, *Rev. Mod. Phys.* **70**, 1003 (1998).

³ Z. Kis and F. Renzoni, *Phys. Rev. A* **65**, 032318 (2002).

⁴ C. Emary and L. J. Sham, *J. Phys.: Condens. Matter* **19**, 056203 (2007).

⁵ R. G. Unanyan, B. W. Shore, and K. Bergmann, *Phys. Rev. A* **63**, 043405 (2001).

⁶ D. Loss and D. P. DiVincenzo, *Phys. Rev. A* **57**, 120 (1998).

⁷ A. Greilich, D. R. Yakovlev, A. Shabaev, Al. L. Efros, I. A. Yugova, R. Oulton, V. Stavarache, D. Reuter, A. Wieck, M. Bayer, *Science* **313**, 341 (2006).

⁸ J. R. Petta, A. C. Johnson, J. M. Taylor, E. A. Laird, A. Yacoby, M. D. Lukin, C. M. Marcus, M. P. Hanson, A.

- C. Gossard, *Science* **309**, 2180 (2005); F. H. L. Koppens, C. Buizert, K. J. Tielrooij, I. T. Vink, K. C. Nowack, T. Meunier, L. P. Kouwenhoven and L. M. K. Vandersypen, *Nature* **442**, 766 (2006).
- ⁹ A. Imamoglu, D. D. Awschalom, G. Burkard, D. P. DiVincenzo, D. Loss, M. Sherwin, and A. Small, *Phys. Rev. Lett.* **83**, 4204 (1999).
- ¹⁰ C. Piermarocchi, Pochung Chen, L. J. Sham, and D. G. Steel, *Phys. Rev. Lett.* **89**, 167402 (2002).
- ¹¹ R. J. Warburton, C. Schflein, D. Haft, F. Bickel, A. Lorke, K. Karrai, J. M. Garcia, W. Schoenfeld and P. M. Petroff, *Nature* **405**, 926 (2000).
- ¹² X. Xu, Y. Wu, Bo Sun, Q. Huang, J. Cheng, D. G. Steel, A. S. Bracker, D. Gammon, C. Emary, and L. J. Sham, *Phys. Rev. Lett.* **99**, 097401 (2007).
- ¹³ M. Atatüre, J. Dreiser, A. Badolato, A. Högele, K. Karrai, and A. Imamoglu, *Science* **312**, 551 (2006).
- ¹⁴ M. Atatüre, J. Dreiser, A. Badolato and A. Imamoglu, *Nature Physics* **3**, 101 (2007).
- ¹⁵ J. Berezovsky, M. H. Mikkelsen, N. G. Stoltz, L. A. Col-dren, D. D. Awschalom, *Science* **320**, 349 (2008).
- ¹⁶ B. D. Gerardot, S. Strauf, M. J. A. de Dood, A. M. Bychkov, A. Badolato, K. Hennessy, E. L. Hu, D. Bouwmeester, and P.M. Petroff, *Phys. Rev. Lett.* **95**, 137403 (2005).
- ¹⁷ M. Scheibner, I. V. Ponomarev, E. A. Stinaff, M. F. Doty, A. S. Bracker, C. S. Hellberg, T. L. Reinecke, and D. Gammon, *Phys. Rev. Lett.* **99**, 197402 (2007).
- ¹⁸ C. Emary and L. J. Sham, *Phys. Rev. B* **75**, 125317 (2007).
- ¹⁹ B. W. Lovett, A. Nazir, E. Pazy, S. D. Barrett, T. P. Spiller, and G. A. Briggs, *Phys. Rev. B* **72**, 115324 (2005).
- ²⁰ S. M. Clark, Kai-Mei C. Fu, T. D. Ladd, and Y. Yamamoto *Phys. Rev. Lett.* **99**, 040501 (2007).
- ²¹ T. Calarco, A. Datta, P. Fedichev, E. Pazy, and P. Zoller, *Phys. Rev. A* **68**, 012310 (2003).
- ²² E. Biolatti, I. D'Amico, P. Zanardi, and F. Rossi, *Phys. Rev. B* **65**, 075306 (2002).
- ²³ C. Emary, Xiaodong Xu, D. G. Steel, S. Saikin, and L. J. Sham, *Phys. Rev. Lett.* **98**, 047401 (2007).
- ²⁴ D. Jaksch, J. I. Cirac, P. Zoller, S. L. Rolston, R. Côté, and M. D. Lukin, *Phys. Rev. Lett.* **85**, 2208 (2000).
- ²⁵ F. T. Hioe and C. E. Carroll, *Phys. Rev. A* **37**, 3000 (1988).
- ²⁶ W. K. Wootters, *Phys. Rev. Lett.* **80**, 2245 (1998).
- ²⁷ J. F. Poyatos, J. I. Cirac, and P. Zoller, *Phys. Rev. Lett.* **78**, 390 (1997).
- ²⁸ C. F. Roos, G. P. T. Lancaster, M. Riebe, H. Hffner, W. Hänsel, S. Gulde, C. Becher, J. Eschner, F. Schmidt-Kaler, and R. Blatt, *Phys. Rev. Lett.* **92**, 220402 (2004).